Special Feature: Vehicle Engineering

Research Report

Four-wheel Active Steering Control Based on Human Sensitivity

Yoshikazu Hattori, Eiichi Ono, Katsuhiko Fukui and Yuji Muragishi

Report received on Nov. 1, 2012

ABSTRACT Target vehicle dynamics to enhance a driver's perception of a vehicle's agility and stability in yaw and lateral motion have been suggested. Human sensitivity is a significant factor in determining such targets. A four-wheel active steering system has the capability to realize these target dynamics effectively.

This paper proposes a control design concept for a four-wheel active steering system on the basis of four representative human sensitivities. These four factors of the vehicle dynamics are essential in order to modify the driver's evaluation for agility and stability in the middle- to high-speed region.

On the other hand, in the low-speed region, the relation between yaw velocity and body slip angle was found to be one of the dominant factors in the driver's perception.

The validity of the proposed target dynamics is then confirmed by the active steering system.

KEYWORDS Vehicle Dynamics, Four Wheel Steering, Active Control, Human Sensitivity

1. Introduction

Active steering control systems have been investigated since the 1980s. Initially, analyses based on control theory were widely attempted, and in the late 1980s, active rear steering control systems came into practical use. In early 2000, an active front steering system was commercialized. The current focus is on active four-wheel steering systems.[1] Active front and rear steering systems extend the regions of feasible vehicle dynamics, thereby facilitating the realization of "ideal" vehicle dynamics.[2,3] The original purpose of the control was to realize theoretically ideal vehicle dynamics using pure control theory; for example, to make the body slip angle zero or to flatten the frequency response between the steering wheel angle and the yaw velocity.[4] However, because automobiles are driven by humans, the driver fulfills the role of both controller and vehicle dynamics evaluator. Therefore, vehicle control systems should also be designed in a manner that takes human characteristics into consideration. In discussing ideal dynamics of automobile steering and cornering, the issue of what the driver feels vs. the physically measurable quantities is raised. In other words, if a vehicle has ideal dynamics, the vehicle motion will be consistent with what the driver expects. However, what the driver "feels" is conveyed to the driver through his or her sensory apparatus.

As part of the research into human characteristics, the well-known findings of Weir et al.[5] indicate the existence of a yaw characteristics region in which drivers perceive driving to be easier. This region is described by the relationship of the steady yaw velocity gain and time lag. Additionally, Abe et al.[6] reported the desirability of variable steering gear-ratio systems that can control the vehicle yaw characteristics depending on the vehicle speed. Previous research has shown that phase-lead control of a front steering system contributes to driver perception of superior vehicle controllability. The results have been applied to commercialized active front steering systems. In parallel with the development of steering control systems, the fundamental characteristics of human motion and visual sensitivities for single direction motion have also been investigated. Furthermore, the scope of this research was enlarged from single to combined motions. Additionally, human evaluation functions with regard to practical vehicle dynamics have also been considered.

The purpose of the present paper is to propose a controller design method and the target vehicle dynamics to which driver sensitivity and evaluation characteristics are applied.

We start the discussion from an investigation into the physical values that drivers perceive for sensing and evaluating vehicle dynamics. This fundamental perceptional characteristic suggests the physical values that the vehicle controller should adjust in the middle- to high-speed range.

In Section 3, we derive a design method of the simplest controller capable of controlling these physical values. Section 4 describes the properly coordinated controller parameters that reflect the driver characteristics. Low-speed cornering is discussed in Sections 5 and 6. In low-speed cornering situations, the vehicle has a relatively large yaw velocity and body slip angle. The body slip angle affects the recognition of rotating speed.

This report discusses how the variation between body slip angle and yaw velocity and their resultant effects affect the driver's perception (or evaluation of the situation) during low-speed cornering.

As the starting point, a maneuverability test for low-speed cornering was conducted for front and rear steering vehicles. The results indicate that the driver can comfortably control this higher-yaw-velocity-gain steering and that a smaller outward body slip angle is generated during low-speed cornering.

Next, the observed characteristics will be investigated through the analysis of the driver-vehicle closed-loop system. The driver is assumed to recognize the angle between the vehicle heading direction and the gaze point as the gaze angle and is assumed to steer based on the first-order look-ahead driver model.

2. Driver Sensitivity to Vehicle Response for Steering

Vehicle dynamics is evaluated based on driver sensitivity and feelings, which essentially means using the driver as a sensor or evaluator in a human-vehicle closed loop system (**Fig. 1**).

For this reason, when vehicle dynamics controllers are designed, it is important to consider driver perception of vehicle dynamics and to make positive efforts to control the dynamics that drivers sense to be important. In planar movement, it is essential to create a good balance between yaw motion and lateral translation based on considerations of driver sensitivity. The balance of characteristics determines the results of evaluations for vehicle dynamics.

The main human sensors for vehicle dynamics are vision and bodily sensations. The dominant sensor for yaw motion is vision, and the dominant sensor for lateral translation is bodily sensation. Additionally, when the driver detects variations in these motions, the main object for visual information is the yaw velocity and the main object for bodily sensation is the lateral jerk.[7] As a result of research regarding sensitivity to yaw velocity and lateral jerk, it was found that the discrimination of yaw velocity is influenced not only by steady-state gain but also by dynamic response.

A driving simulator equipped with view screens and motion actuators was used for this research. The front view depicted in **Fig. 2** was shown to the test subjects, and the driving task was a slalom course.

Yaw velocity as a function of steering wheel angle for the driving simulator was based on the following equation.

$$\gamma = \frac{K_\gamma}{1+sT_s}\delta_{MA}, \quad \cdots\cdots\cdots\cdots\cdots\cdots\cdots\cdots (1)$$

where γ is the yaw velocity, K_γ is the steady gain

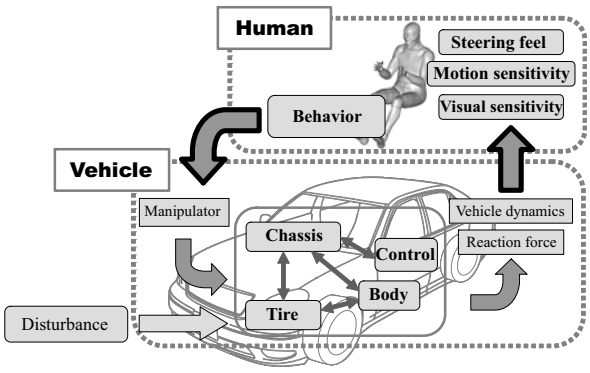

Fig. 1 Evaluation in a human-vehicle loop system.

Fig. 2 Driving task.

between the steering wheel angle and yaw velocity, T_s is the lag, δ_{MA} is the steering angle, and s is the Laplace operator. Furthermore, the vehicle slip angle was always zero, and the vehicle speed was constant. The driving task was to follow a slalom course. The slalom interval was the length of the dashed lines, as shown by the arrow in Fig. 2. A paired comparison test was performed between reference characteristics and actual characteristics, which were varied corresponding to sets of steady gain and lag. The subjects were asked to choose an answer from among three alternatives for vehicle response: faster/same/smaller. The experimental result are shown in **Fig. 3**.

When the lag was the same as the reference, the threshold at which the drivers perceived an increase in steady-state yaw gain (i.e., 'faster') was 120% of the reference yaw gain. On the other hand, when $T_s = 0.05$, the test subjects answered that the yaw motion was larger than the reference yaw, despite the yaw gain being the same. That is to say that a smaller lag time reduces the threshold for discrimination. As a result, it is difficult for a driver to evaluate the magnitude of yaw gain while separating steady gain from the response.

Furthermore, the magnitude and generation timing of lateral jerk is also important for the desirability of the vehicle lateral motion.[8]

The above paragraph discussed the sensitivity for individual direction dynamics. This paragraph considers the driving criteria based on combined sensitivity in cornering including both lateral translation and yaw rotation. **Figure 4** shows two kinds of reference steady yaw velocity gain K_γ^*, which were evaluated as a controllable value by test drivers. One was obtained from the driving simulator, where the driver was given only visual information. The other was obtained from driving a real vehicle, where the driver was able to receive both visual and motion information. Note that the two kinds of K_γ^* exhibit different distributions. The results in the driving simulator were approximately constant, regardless of the vehicle speed. On the other hand, the results in the real vehicle exhibited a different trend, especially in the higher-speed region. The following paragraph discusses the cause of this difference.

Figure 5 displays the perceptible thresholds of vision and bodily sensation for each direction of translation and rotation. The figure shows that vision has a smaller threshold than bodily sensation for yaw velocity, and that bodily sensation has a smaller threshold than vision for lateral translation.[9]

Figure 6 focuses on the smallest yaw velocity amplitude of the yaw velocity or lateral jerk approach

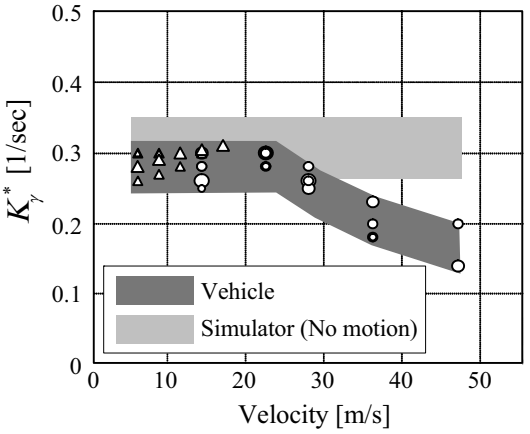

Fig. 4 Evaluation for yaw gain.

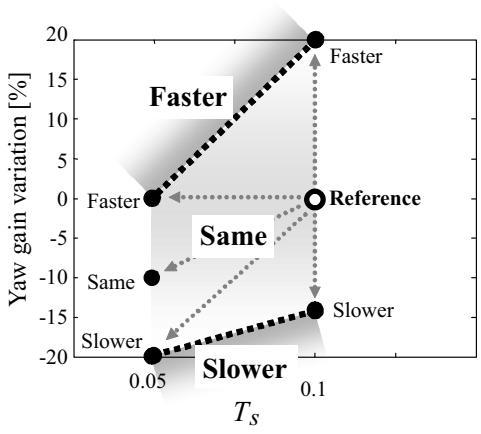

Fig. 3 Driver sensitivity to dynamics.

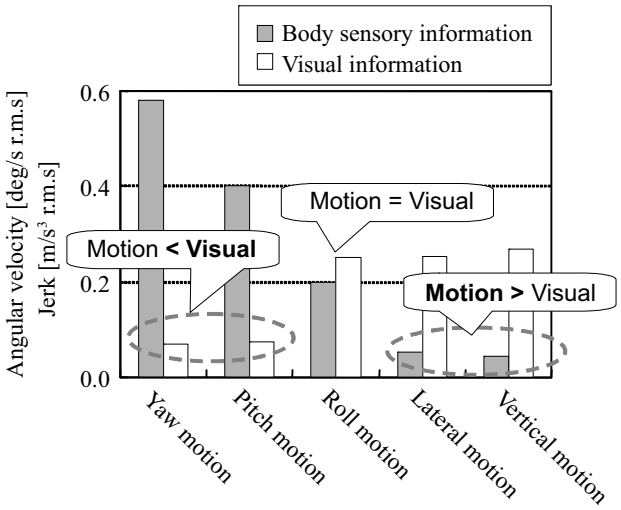

Fig. 5 Perception sensitivity for each motion.

with regard to the perceptible thresholds corresponding to vehicle speed while cornering. In the figure, ε_γ, ε_{dGy} are the perceptible thresholds for yaw velocity and lateral jerk, respectively, and the driving task was a slalom course with a constant frequency of $\omega = \pi$ [rad/s].

The yaw velocity amplitude when the lateral jerk amplitude approaches the perceptible threshold is inversely proportional to the vehicle speed, as shown by the following equation.

$$\gamma_{\epsilon_{dG_y}} = \frac{\epsilon_{dG_y}}{\omega v} \quad \cdots\cdots\cdots\cdots\cdots\cdots\cdots\cdots (2)$$

On the othe hand, the yaw velocity is perceptible on the constant threshold $\in_\gamma$ regardless of the vehicle speed. Consequently, in the low-speed region, the yaw velocity is perceptible in smaller motions than lateral jerk. However, lateral jerk is perceptible at a lower threshold than the yaw velocity in the high-speed region. Therefore, the vehicle speed at which the perceptible priority switches between the yaw velocity and lateral jerk is about 15 to 25 m/s, although this depends on variations in the perceptible threshold.

Considering that the evaluation for vehicle motion is based on perception and discrimination, the results of Fig. 6 support the hypothesis that drivers evaluate cornering motion based on lateral jerk in the high-speed region and based on yaw velocity in the low-speed region. Accordingly, the isosensitivity criteria, which indicate that drivers prefer to feel equal gain through a driving situation, can be used to establish vehicle dynamics compatible with driver perception. The isosensitivity curve of yaw gain is shown in **Fig. 7** over the entire speed range.

Its shape implies that beyond the perception priority threshold of 15 to 25 m/s, the yaw rate gain should diminish to achieve driver perception of constant yaw gain. This means that lateral jerk characteristics should be regarded as important in controller designs for vehicle operation at higher speeds. The results obtained from the driving simulator support this assumption. That is to say, constant yaw characteristics over all speed ranges are desirable based only on yaw velocity since drivers were unable to evaluate bodily sensitivity in the driving simulator.

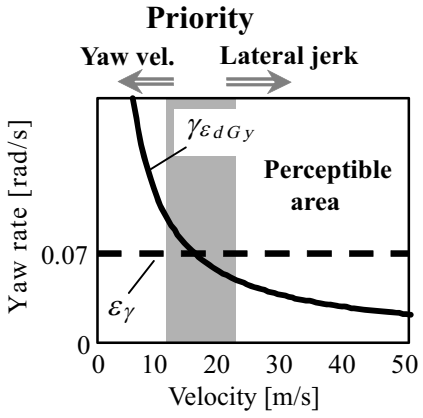

Fig. 6 Perception priority.

3. Control Design of Four-wheel Active Steering Based on Human Sensitivity

As described above, the characteristics of yaw velocity and lateral jerk are important for the design of cornering characteristics. Furthermore, the magnitude of yaw motion felt by the driver can be controlled using both steady gain and response time. Additionally, it is obvious from previous research that the body slip angle is also an important factor. This section proposes a control design method for an active four-wheel steering system based on human sensitivity. The proposed method can directly adjust the vehicle dynamics characteristics noticed by the driver as the target value.

A linear half car model with front and rear steering was formulated as follows.

$$\begin{cases} mv\left(\dfrac{d\beta}{dt}+\gamma\right) = -2K_f\alpha_f - 2K_r\alpha_r \\ I_z\dfrac{d\gamma}{dt} = -2K_f\alpha_f l_f + 2K_r\alpha_r l_r \end{cases}, \quad \cdots\cdots\cdots\cdots\cdots (3)$$

where β is the body slip angle, γ is the yaw velocity, I_z is the yaw inertia, K_f and K_γ are the front and rear

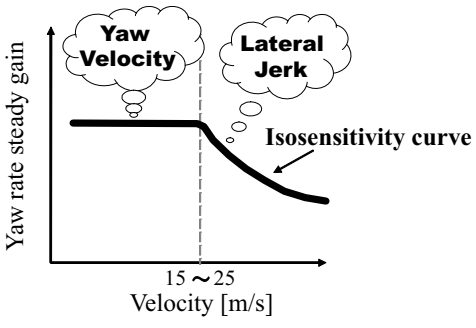

Fig. 7 Isosensitivity criteria.

cornering stiffness, m is the vehicle mass, l is the wheelbase, l_f and l_r are the distances between the front and rear wheel axes and the center of gravity, respectively, v is the vehicle speed, and α_f and α_r are front and rear tire slip angles, respectively, as formulated by the follow equation.

$$\begin{cases} \alpha_f = \beta + \dfrac{l_f}{v}\gamma - \delta_f \\ \alpha_r = \beta - \dfrac{l_r}{v}\gamma - \delta_r \end{cases}, \quad \cdots\cdots\cdots\cdots\cdots (4)$$

where δ_f , δ_r are the front and rear steering angles, respectively. Equation (5) is obtained by the Laplace transform of Eq. (3).

$$\begin{bmatrix} \beta \\ \gamma \end{bmatrix} = \frac{1}{\Delta_s(s)} \begin{bmatrix} N_1(s) & N_2(s) \\ N_3(s) & N_4(s) \end{bmatrix} \begin{bmatrix} \delta_f \\ \delta_r \end{bmatrix}, \quad \cdots\cdots\cdots (5)$$

where s is the Laplace operator, $\Delta_s(s)$ is the characteristics equation of the half car mode shown by Eq. (6) below, and N_1 through N_4 are the numerators of the plant formulated as Eqs. (7) through (10) below.

$$\Delta_s(s) = s^2 + \frac{2\left(I_z\left(K_f + K_r\right) + m\left(l_f^2 K_f + l_r^2 K_r\right)\right)}{mvI_z} s + \frac{4l^2 K_f K_r - 2mv^2\left(l_f K_f - l_r K_r\right)}{mv^2 I_z} \quad \cdots\cdots\cdots\cdots (6)$$

$$N_1 = \frac{2K_f\left(2ll_r K_r - mv^2 l_f\right)}{mv^2 I_z} + \frac{2K_f}{mv} s \quad \cdots\cdots (7)$$

$$N_2 = \frac{2K_r\left(2ll_f K_f + mv^2 l_r\right)}{mv^2 I_z} + \frac{2K_r}{mv} s \quad \cdots\cdots (8)$$

$$N_3 = \frac{4lK_f K_r}{mvI_z} + \frac{2l_f K_f}{I_z} s \quad \cdots\cdots\cdots\cdots (9)$$

$$N_4 = -\frac{4lK_f K_r}{mvI_z} - \frac{2l_r K_r}{I_z} s \quad \cdots\cdots\cdots\cdots (10)$$

Now, considering that the yaw response is adjusted by the differential term γ_1^* and that the steady gain is adjusted by $\gamma_0^*(=\gamma_0^{*'}/\Delta_s(0))$, γ^* in the following equation is defined as the target yaw velocity.

$$\gamma^* = \frac{\gamma_0^{*'}\left(1 + s\,\gamma_1^*(s)\right)}{\Delta_s(s)} \delta_{MA} \quad \cdots\cdots\cdots\cdots (11)$$

Next, the lateral jerk is formulated as follows.

$$dG_y = v\left(s^2\beta + s\gamma\right) \quad \cdots\cdots\cdots\cdots (12)$$

Furthermore, the initial rise characteristics of dG_y depend on the highest-order term of the numerator. The highest-order term is denoted by J_H^* . Finally, adding the slip angle steady gain $\beta_0^*(=\beta_o^{*'}/\Delta_s(0))$, the above four parameters, γ_0^*, γ_1^*, J_H^*, β_0^* are decided as the target characteristics. Accordingly, the subject here is to construct a design method for an active four-wheel steering controller that can adjust the above four parameters to any values.

The front and rear steering controllers are denoted by $C_1(s)$, $C_2(s)$, respectively. The input is the steering wheel angle, and the outputs are the target steering angle of the front and rear wheels. Here, C_1 and C_2 are constructed by the proportional terms C_{10}, C_{20}, and the differential terms $C_{11}(s)$ and $C_{21}(s)$, which have the numerators $N_3(s)$ and $N_4(s)$ as the denominators of the controller. Consequently, C_{10}, C_{20}, C_{110}, and C_{210} are constant gains and determine the four parameter values for each steering controller. These values are obtained by gain maps corresponding to the vehicle speed (**Fig. 8**). The differential filters in Fig. 8 are $s/N_3(s)$ and $s/N_4(s)$, respectively. The point is to have the numerator of the plant system as the denominator.

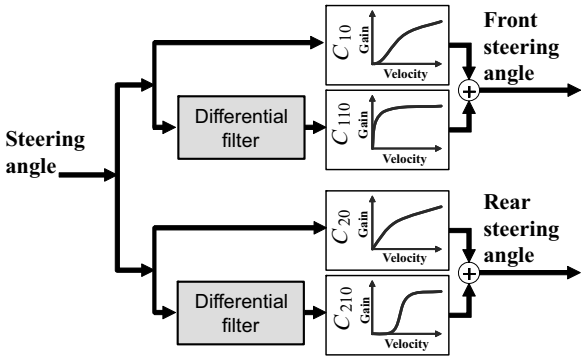

Fig. 8 Controller structure.

$$\begin{aligned}\delta_f &= C_1(s)\,\delta_{MA}\\ &= \left(C_{10}+C_{11}(s)\right)\delta_{MA}\\ &= \left(C_{10}+\frac{s}{N_3(s)}C_{110}\right)\delta_{MA}\end{aligned} \quad \cdots\cdots\cdots (13)$$

$$\begin{aligned}\delta_r &= C_2(s)\,\delta_{MA}\\ &= \left(C_{20}+C_{21}(s)\right)\delta_{MA}\\ &= \left(C_{20}+\frac{s}{N_4(s)}C_{210}\right)\delta_{MA}\end{aligned} \quad \cdots\cdots\cdots (14)$$

Equation (16) is obtained by substituting Eqs. (13) and (14) into Eq. (5). Here, if N_i and N_i' : (i = 1 through 4) are represented as Eq. (15), Eq. (5) can be solved as shown in Eq. (24).

$$N_i(s) = N_i(0) + sN_i' \quad \cdots\cdots\cdots (15)$$

$$\begin{bmatrix}\beta\\ \gamma\end{bmatrix} = \frac{1}{\Delta_s(s)}\begin{bmatrix}N_1(s) & N_2(s)\\ N_3(s) & N_4(s)\end{bmatrix}\begin{bmatrix}C_{10}+\frac{s}{N_3}C_{110}\\ C_{20}+\frac{s}{N_4}C_{210}\end{bmatrix}\delta_{MA} \quad \cdots\cdots\cdots (16)$$

$$\begin{aligned}&= \frac{1}{\Delta_s(s)}\begin{bmatrix}N_1(0) & N_2(0)\\ N_3(0) & N_4(0)\end{bmatrix}\begin{bmatrix}C_{10}\\ C_{20}\end{bmatrix}\delta_{MA}\\ &+ \frac{s}{\Delta_s(s)}\begin{bmatrix}N_1' & N_2'\\ N_3' & N_4'\end{bmatrix}\begin{bmatrix}C_{10}\\ C_{20}\end{bmatrix}\delta_{MA}\\ &+ \frac{s}{\Delta_s(s)}\begin{bmatrix}\frac{N_1(s)}{N_3(s)} & \frac{N_2(s)}{N_4(s)}\\ 1 & 1\end{bmatrix}\begin{bmatrix}C_{110}\\ C_{210}\end{bmatrix}\delta_{MA}\ , \quad \cdots (17)\end{aligned}$$

where the first term of Eq. (17) corresponds to the steady gain of the body slip angle and yaw velocity (β_0^*, γ_0^*) expressed as follows.

$$\begin{bmatrix}\beta_0^*\\ \gamma_0^*\end{bmatrix}\delta_{MA} = \frac{1}{\Delta_s(0)}\begin{bmatrix}N_1(0) & N_2(0)\\ N_3(0) & N_4(0)\end{bmatrix}\begin{bmatrix}C_{10}\\ C_{20}\end{bmatrix}\delta_{MA} \quad \cdots\cdots\cdots (18)$$

By solving the above equations, the proportional gain of the controller is obtained as follows.

$$C_{10} = \beta_0^* + \frac{1}{2}\frac{2ll_fK_f + mv^2l_r}{vlK_f}\gamma_0^* \quad \cdots\cdots\cdots (19)$$

$$C_{20} = \beta_0^* - \frac{1}{2}\frac{2ll_rK_r - mv^2l_f}{vlK_r}\gamma_0^* \quad \cdots\cdots\cdots (20)$$

Next, sorting the factor of yaw velocity in Eq. (16) by applying C_{10}, C_{20} and $\gamma_0^{*'}$, γ_1^* in Eq. (11), Eq. (21) is derived as follows.

$$C_{110} + C_{210} = \gamma_0^{*'}\gamma_1^* - \left(N_3'C_{10} + N_4'C_{20}\right) \quad \cdots\cdots (21)$$

Finally, it is necessary to consider the rise characteristics of lateral jerk. Focusing on the body slip angle part from Eq. (16) and sorting the second term of Eq. (17) as $\beta_{p0} \equiv N_1'\,C_{10} + N_2'\,C_{20}$, Eq. (23) is obtained.

$$\begin{aligned}\beta = \frac{1}{\Delta_s(s)}&\left(\beta_0^{*'} + s\,\beta_{p0}\right.\\ &\left. + s\left(\frac{N_1(s)}{N_3(s)}C_{110} + \frac{N_2(s)}{N_4(s)}C_{210}\right)\right)\delta_{MA}\end{aligned} \quad \cdots\cdots\cdots (22)$$

$$\begin{aligned}&= \frac{1}{\Delta_s(s)N_3(s)N_4(s)}\\ &\left\{N_3(s)N_4(s)\beta_0^{*'} + s\left(N_3(s)N_4(s)\beta_{p0}\right.\right.\\ &\left.\left. + N_1(s)N_4(s)C_{110} + N_2(s)N_3(s)C_{210}\right)\right\} \quad \cdots (23)\end{aligned}$$

By substituting Eqs. (7) through (10) and (15) into Eq. (23), the highest-order term of the numerator J_H of the right-hand side is expressed by Eq. (24), which is regarded as the target characteristics of lateral jerk J_H^*.

$$\begin{aligned}J_H^* = &-\frac{4K_fK_r}{mvI_z}\left(l_rC_{110} - l_fC_{210}\right)\\ &-\frac{8K_fK_rl_fl_r}{mvI_z^2}\left(K_fC_{10} + K_rC_{20}\right)\ , \quad \cdots\cdots (24)\end{aligned}$$

where $N_3(s) > 0$ from Eq. (9) and $N_4(s) > 0$ from

Eq. (10). Therefore, the denominator of the right-hand side of Eq. (23) is negative. Accordingly, J_H^* becomes smaller, the feedthrough term becomes larger, and the response becomes quicker. As C_{10} and C_{20} have already been determined by Eqs. (19) and (20), $(l_r C_{110} - l_f C_{210})$ should be taken as a large value for quick response of lateral jerk. If $(l_r C_{110} - l_f C_{210})$ is determined by the desired lateral jerk, C_{110} and C_{210} can be specified because $(C_{110} + C_{210})$ is given by Eq. (21).

As described above, the four controllers shown in Fig. 8 corresponding to γ_0^*, β_0^*, γ_1^*, and J_H^*, which depend on vehicle speed, can be determined by Eqs. (18), (21), and (24).

4. Verification Experiments Using a Real Vehicle

The realized vehicle characteristics, γ_0^*, β_0^*, γ_1^*, and J_H^* are adjusted by the proposed control method based on sensory evaluation corresponding to vehicle speed, as follows. **Figure 9** indicates the relationship between vehicle speed and steady gain of yaw velocity. The proposed method (A-4WS) has a higher gain in the lower-speed region and a lower gain in the higher-speed region than the conventional vehicle (2WS). The shaded line indicates the isosensitive curve shown in Fig. 7 and shows that the value of the proposed method is flatter than the isosensitive curve, corresponding to the vehicle speed.

On the other hand, focusing on the phase characteristics between the steering wheel angle and yaw velocity in a 0.5 Hz slalom course (**Fig. 10**), the phase of A-4WS is ahead in the lower-speed region and behind in the higher-speed region, as compared to 2WS. Consequently, the yaw gain of A-4WS is different from the physical isosensitivity characteristics as shown in Fig. 9. However, the yaw gain is modified approaching the isosensitivity curve with regard to driver sensitivity by adjusting the phase characteristics.

In the case of a real vehicle, there are cases in which a steady yaw gain cannot be applied to the isosensitivity curve due to various constraints. For example, when decelerating with a fixed steering angle out of a corner with a constant radius, a vehicle with a yaw gain on the isosensitivity curve will turn toward the inside due to increases in the yaw velocity. Such characteristics are not acceptable in normal passenger vehicles. Thus, the proposed controller has two methods, i.e., the steady yaw gain γ_0^* and differential gain γ_1^*, to adjust the yaw characteristics. Therefore, the controller can make the sensory yaw characteristics approach the isosensitivity criteria, which means that the proposed controller can achieve the desired yaw characteristics over a wider region under various constraints.

The difference in initial lateral jerk between A-4WS and 2WS is shown in **Fig. 11**. In this case, the vehicle was steered by a steering robot with sine wave

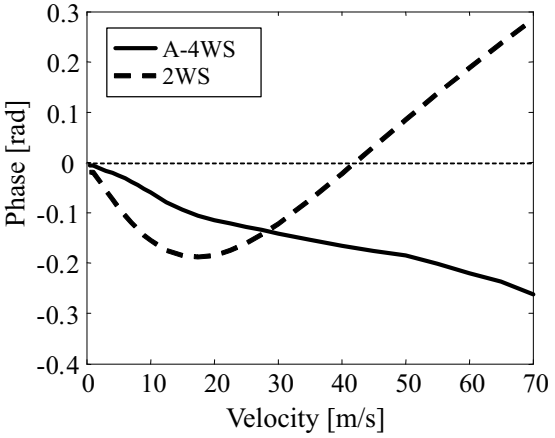

Fig. 10 Phase of yaw velocity @ f = 0.5 Hz.

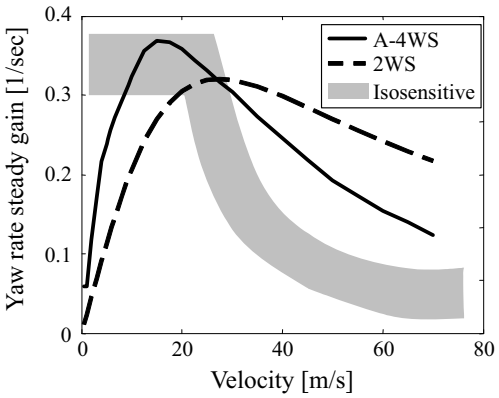

Fig. 9 Yaw characteristics.

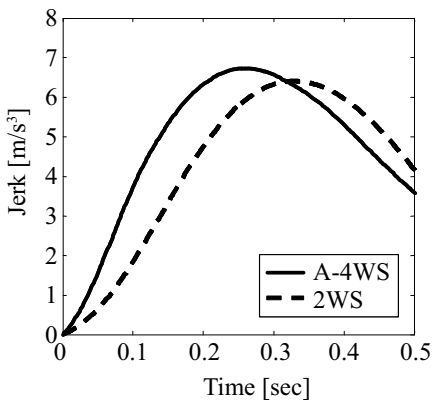

Fig. 11 Lateral jerk response.

characteristics with a frequency of 0.5 Hz. The amplitude of lateral acceleration was 0.25 G. According to previous research,[8] the driver feels a sense of stability when the timing of the lateral jerk peak is faster and the maximum value is larger. Figure 11 indicates that A-4WS gives the driver a perception of higher stability. Additionally, the targets for the front and rear steering angles are shown in **Fig. 12**, and the tire slip angles shown in **Fig. 13** are normalized by each maximum value for easier understanding. The phase of both of the controlled front and rear steering angles is in advance of the steering wheel angle. The phase-lead control contributes to quick response of lateral jerk.

5. Sensory Evaluation of Rotating Velocity During Low-speed Cornering

The active front and rear steering system can produce a range of characteristics of vehicle dynamics with various combinations of body slip angle and yaw velocity. Sensory evaluation of the rotating velocity felt by the driver during low-speed cornering was performed. The driving course is shown in **Fig. 14**.

The test subjects are three skilled drivers. In the examination, the subject drivers were instructed to adjust the vehicle speed to 5 m/s. The subjects evaluated and reported the rotating speed that they felt. The results are indicated in **Table 1**. We provided an appropriate explanation to the subjects before the examination and obtained consent from the subjects.

Representative examples of comments are shown in Table 1. Note that when two vehicles with different gains from the steering wheel to body slip angle or yaw velocity $\{\beta_0', \gamma_0'\}$ or $\{\beta_0'', \gamma_0''\}$ drive on the same course at the same speed, if the gains of the two vehicles satisfy the following equation, the body slip angles of the vehicles are equal during cornering. Thus, γ_0 and β_0/γ_0 (normalized slip angle gain) were adopted as the parameters in Table 1.

$$\frac{\beta_0'}{\gamma_0'} = \frac{\beta_0''}{\gamma_0''} \quad \cdots\cdots\cdots\cdots\cdots\cdots\cdots\cdots (25)$$

The results of the sensory evaluation are displayed in **Fig. 15**. In low-speed tight cornering, higher-yaw-

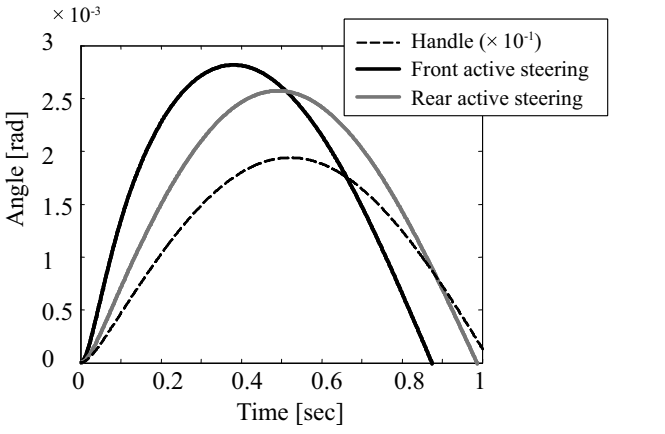

Fig. 12 Active steering angles.

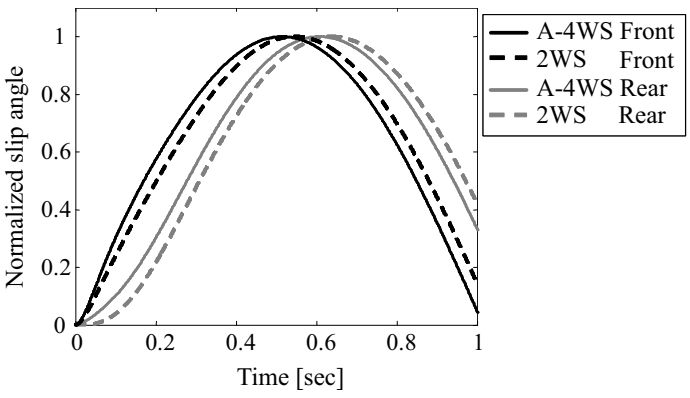

Fig. 13 Normalized tire slip angles.

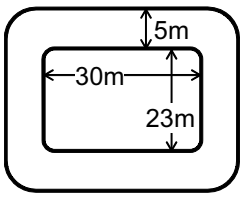

Fig. 14 Driving course.

Table 1 Sensory evaluation.

test no.	vehicle char. γ_0	vehicle char. $\frac{\beta_0}{\gamma_0}$	evaluation	comments
1	1.7001	0.2798	○	busy(2WS)
2	3.2579	0.2798	×	too sensitive
3	2.5348	0.2798	○	acceptable
4	2.7460	0.2798	○	good
5	2.44	0.2008	○	acceptable
6	2.928	0.2008	○	acceptable
7	3.416	0.2008	×	too sensitive
8	3.65	0.0799	×	tea-cup feeling

velocity gain tends to be desirable. The reason would be that drivers can use a smaller steering angle. However, for high gain this causes an unusually sensitive response from the vehicle. Subjects commented that they had a threshold for acceptable yaw gain.

The examination result showed that a smaller normalized slip angle gain made the driver accept a larger yaw velocity gain. The threshold value of acceptable yaw velocity gain has an individual difference. However, the feature whereby smaller body slip gain makes a larger yaw velocity gain acceptable was observed for all of the subject drivers (**Figs**. 15 and **16**).

On the other hand, if the slip angle gain is too small, another uncomfortable sensation referred to as the "tea cup feeling" is induced. This sensation resembles the feeling experienced when riding on a "tea cup" attraction at an amusement park, which causes the rider to experience extremely tight rotation. Over-rotating motions appear to generate this sensation.

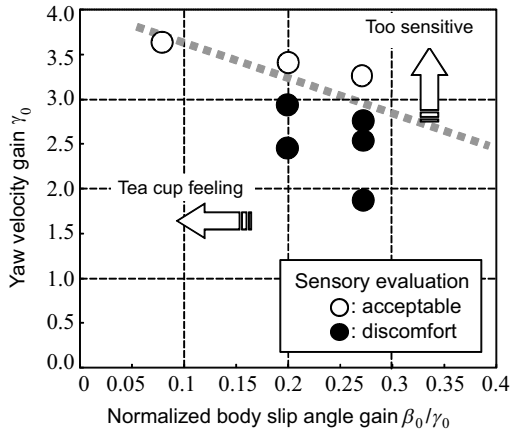

Fig. 15 Driver's feeling for vehicle characteristics.

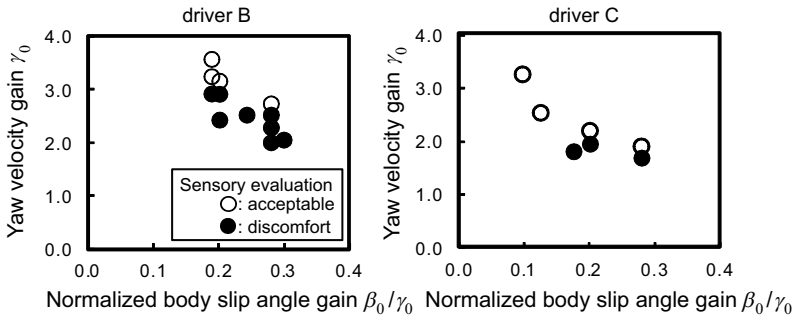

Fig. 16 Driver's feeling for vehicle characteristics: other drivers.

6. Consideration Based on the Human-vehicle Closed Loop

In the preceding section, we focused on the relationship between the normalized slip angle gain and acceptable yaw velocity gain. One aspect of the characteristic is obtained analytically using a driver model.

6. 1 Driver Model

[Look-ahead driver model]

A look-ahead driver model is used as a path-following controller. Various driver models have been proposed. The present study uses the following driver model,[10] which is one of the simplest first-order look-ahead driver models.

The driver model feeds back the gaze angle $\theta_{gaze}(t)$ between a gaze point of L ahead and the current traveling direction of vehicle (**Fig. 17**) and outputs the yaw velocity of the vehicle $\gamma(t)$ (Eq. (26)). The vehicle is considered to be a point mass, so the yaw velocity is defined as the rotating speed of the vehicle traveling vector.

$$\gamma(t) = K_m \theta_{gaze}(t - \tau_m) \quad \cdots\cdots\cdots\cdots\cdots (26)$$

The advantage of this model is that the driver model can trace any clothoid curve accurately, despite its simple structure, which consists of dead time τ_m and proportional gain K_m, where the feedback gain K_m and the dead time τ_m can be decided according to only one parameter, predictive time T_m, which is defined by Eq. (27).

$$T_m = \frac{L}{v} \quad \cdots\cdots\cdots\cdots\cdots\cdots\cdots\cdots (27)$$

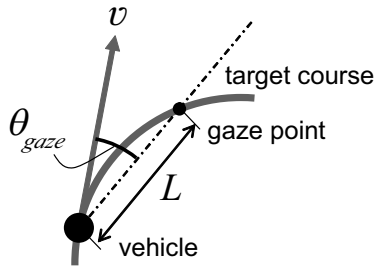

Fig. 17 Course trace control by look-ahead model.

K_m and τ_m are calculated by Eqs. (28) and (29).

$$K_m = \frac{2}{T_m} \quad \cdots\cdots (28)$$

$$\tau_m = \frac{T_m}{3} \quad \cdots\cdots (29)$$

[Closed-loop system with the driver model]

The closed-loop system with the driver model is shown in **Fig. 18**. Here, K_D is the feedback gain from the driver's gaze angle to the steering wheel angle, τ_D is the dead time when the driver drives on a path-following control, δ_{MA} is the steering wheel angle, γ is the yaw velocity of the vehicle, γ_0 is the steady yaw velocity gain of the vehicle, and G_v is the dynamics term of the yaw transition function divided the yaw velocity transition function described in the second row of Eq. (5) by γ_0.

The relationship between the steering wheel angle δ_{MA} and the yaw velocity γ is shown by the next equation.

$$\gamma = \gamma_0 G_v(s)\delta_{MA} \quad \cdots\cdots (30)$$

$$G_v(0) = 1 \quad \cdots\cdots (31)$$

If we approximate G_v by Eq. (32) and the driver operation is expressed by the look-ahead driver model, then, according to Eqs. (26) and (30), K_D and τ_D satisfy the following equations.

$$G_v \approx e^{-s\tau_v} \quad \cdots\cdots (32)$$

$$K_m = \gamma_0 K_D \quad \cdots\cdots (33)$$

$$e^{-s\tau_m} = e^{-s\tau_v} e^{-s\tau_D} \quad \cdots\cdots (34)$$

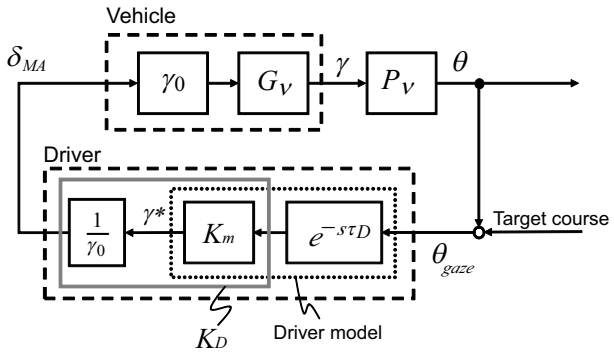

Fig. 18 Block diagram of course trace control.

6. 2 Discussion about the Relationship between Body Slip Angle and the Desired Yaw Velocity Gain

Human beings evaluate physical information caused by vehicle motion through their senses. Therefore, a key point in analyzing vehicle motion is not simply how the vehicle moves, but how the driver perceives that motion. The motion sensibility of the driver should be sufficiently considered.

In the aforementioned driver model, the vehicle is considered to be a point mass. Therefore, the effect of the vehicle heading is dropped, and the angle between the gaze point and the vehicle traveling direction is used as the input value of the controller.

When the driver recognizes the motion of the vehicle, the relative motion as perceived between the front view and various vehicle body parts, such as the instrument panel or the A-pillar, influences his or her overall perception.[11]

A normal automobile has an outward-looking body slip angle during low-speed cornering. Accordingly, the perception of the gaze angle, which is the feedback value for the driver to follow a target path, is expected to also be affected by the vehicle heading. The latter is one of the references for recognizing the vehicle motion.

Therefore, the following hypothesis is introduced and discussed.

> [Hypothesis 1] Driver steers based on the angle between the vehicle heading and the gaze point to trace a target path.

As shown in **Fig. 19**, the angle between the vehicle heading and the gaze point is indicated by θ'_{gaze}.

Let us next consider applying the above driver model to the path-following control of the vehicle with steady yaw velocity gain β_0. Here, the path is assumed to be a circle in order to simplify the discussion.

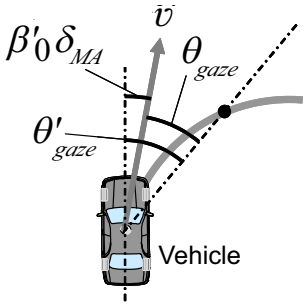

Fig. 19 Gaze angle on vehicle.

The relation between θ_{gaze} and θ'_{gaze} for steady circular driving is as follows.

$$\theta'_{gaze} = \theta_{gaze} + \beta_0 \delta'_{MA}, \quad \cdots\cdots (35)$$

where δ'_{MA} is the steering angle while driving the circle.

If the vehicle with steady yaw velocity gain γ_0 can follow a circle of radius R, the next equations are satisfied.

$$\delta'_{MA} = \frac{v}{R}\frac{1}{\gamma_0} \quad \cdots\cdots (36)$$

$$\sin\theta_{gaze} = \frac{L}{2R} \simeq \theta_{gaze} \quad \cdots\cdots (37)$$

Accordingly, the next equation is obtained from Eqs. (35) through (37):

$$\theta'_{gaze} = \left(1 + \frac{2v}{L}\frac{\beta_0}{\gamma_0}\right)\theta_{gaze}. \quad \cdots\cdots (38)$$

As stated previously, the controller based on Eq. (26) with input value θ_{gaze} can follow any clothoid curve. Next, let us consider replacing the controller input value θ_{gaze} with θ'_{gaze}.

The next equation is obtained by substituting Eq. (38) into Eq. (26).

$$\gamma = K_m\theta_{gaze} = \frac{2}{T_m}\theta_{gaze} = \frac{2}{T_m}\left(1 + \frac{2v}{L}\frac{\beta_0}{\gamma_0}\right)^{-1}\theta'_{gaze}, \quad \cdots\cdots (39)$$

Additionally, each steady value of yaw velocity and steering wheel angle satisfies the next equation.

$$\gamma = \gamma_0\delta'_{MA} \quad \cdots\cdots (40)$$

Consequently, if the steering wheel angle is decided by the next equation using the gaze angle θ'_{gaze} as the controller input value,

$$\delta'_{MA} = K_D\theta'_{gaze}, \quad \cdots\cdots (41)$$

when K_D satisfies the next equation, the vehicle can exactly follow the target circle.

$$K_D = \frac{2v}{\gamma_0 L}\left(1 + \frac{2v}{L}\frac{\beta_0}{\gamma_0}\right)^{-1} \quad \cdots\cdots (42)$$

K_D of Eq. (42) can be regarded as the driver's controller gain from θ'_{gaze} to the steering wheel angle following the path.

Let us next consider how the driver feels the vehicle rotating speed response to steering.

[Hypothesis 2] The driver feels the vehicle rotating speed by the perceived gaze angle response to the steering (**Fig. 20**).

Here, the perceived rotating speed under the foregoing hypotheses γ_0^+ is described by the next equation.

$$\gamma_0^+ = K_D^{-1} = \frac{\gamma_0 L}{2v}\left(1 + \frac{2v}{L}\frac{\beta_0}{\gamma_0}\right) \quad \cdots\cdots (43)$$

Figure 21 shows the relationship between γ_0^+ and the sensory evaluations, where the vehicle speed is 5 m/s and the look-ahead distance is 9 m.

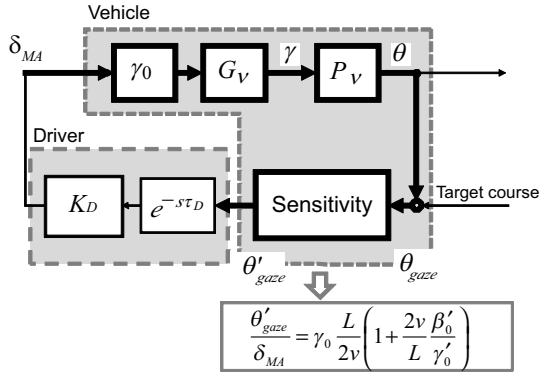

Fig. 20 Plant system for driver.

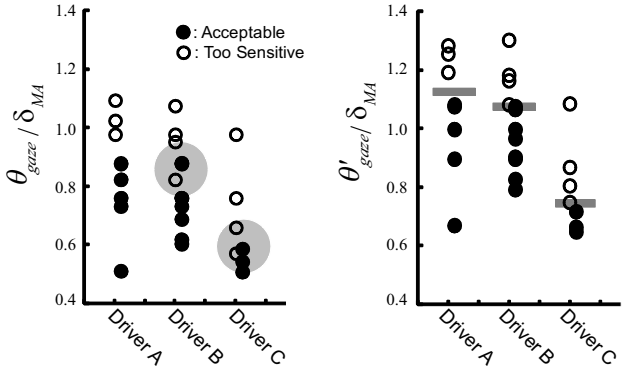

Fig. 21 Threshold of plant gain.

When $\theta_{gaze}/\delta_{MA}$ is used, the acceptable and too-sensitive regions overlap. However, when $\theta'_{gaze}/\delta_{MA}$ is used, these regions are separate, although the thresholds are different.

Figure 22 shows a contour plot of γ_0^+ as calculated by Eq. (43). This plot is superimposed on Fig. 15. Figure 22 indicates that the smaller normalized body slip angle gain makes the driver feel that the vehicle has an equal rotating speed for the larger yaw velocity gain.

Test cases 4 and 6 have the largest values of γ_0, 0.28 and 0.20, respectively, for the acceptable yaw velocity gain for each normalized body slip angle. These cases are plotted along the same contour line. The value of γ_0^+ for these cases is defined as γ_0^*.

As γ_0^+ becomes larger, the driver can follow the path using a smaller steering wheel angle, which makes the driver feel that the vehicle rotating speed is fast. From the viewpoint of manipulating a load, it is better for the driver to be able to follow the path using a smaller steering wheel angle. However, a steering wheel angle that is too small requires more accurate control due to oversensitivity. Consequently, γ_0^+ has a desired value, γ_0^*, which appears to be the most desirable in the situation.

7. Conclusion

This paper has described driver perception in evaluating vehicle motion. An active four-wheel steering system has an essential advantage as a system for modifying targeted vehicle dynamics to be compatible with a driver's perception of desirable dynamics. A control design method focusing on sensory vehicle dynamics was proposed. In the future, the control design method should be expanded to consider human sensitivity in other driving situations.

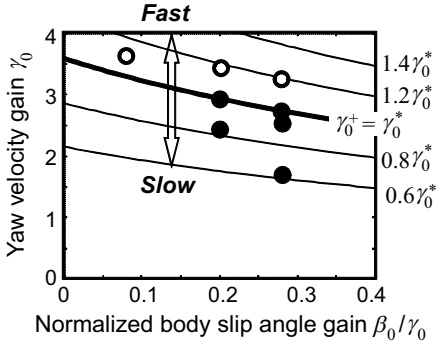

Fig. 22 Driver's sensitivity for yaw velocity gain.

References

(1) Ono, E., et al., "Vehicle Dynamics Integrated Control for Four-wheel-distributed Steering and Four-wheel-distributed Traction/braking Systems", *Vehicle System Dynamics*, Vol. 44, No. 2 (2006), pp. 139-151.
(2) Fujishiro, T., et al.,"Four-wheel Steering System Employing Model-following Control", *Journal of JSAE* (in Japanese), Vol. 42, No. 3 (1988), pp. 304-310.
(3) Sugasawa, F., et al., "Improvements in Vehicle Control and Stability through Front-and Rear-wheel Steering Control", *Transactions of JSAE* (in Japanese), No. 38 (1988), pp. 62-70.
(4) Sugasawa, F., et al., "Improvements in Vehicle Control and Stability through Front-and Rear-wheel Steering Control", *Transactions of JSAE* (in Japanese), No. 38 (1988), pp. 62-70.
(5) Weir, D. H., et al., "Correlation and Evaluation of Driver/Vehicle Directional Handling Data", *SAE Tech. Pap. Ser*., No. 780010 (1978).
(6) Abe, M., et al., "121 Analysis on Steering Gain and Vehicle Handling Performance with VGS (Variable Gear-ratio Steering System)", *JSAE Proceedings* (in Japanese), No. 90-99 (1999), pp. 5-8.
(7) Kodaira, T., et al., "Improvement of Vehicle Dynamics Based on Human Sensitivity (Second Report): A Study of Cornering Feel", *SAE Tech. Pap. Ser*., No. 2007-01-0447 (2007).
(8) Kodaira, T., et al., "Vehicle Transient Response Based on Human Sensitivity", *SAE Tech. Pap. Ser*., No. 2008-01-0597 (2008).
(9) Kodaira, T., et al., "Enhancement of Vehicle Dynamic Behavior Based on Visual and Motion Sensitivity (Third Report): A Sutudy of Pitch", *JSAE Proceedings* (in Japanese), No. 103-06 (2006), pp. 1-4.
(10) Ono, E., et al., "Similarities between Bat Flight and Driver-operated Vehicle Trajectories and Their Unified Model", *Transactions of JSAE* (in Japanese), Vol. 42, No. 6 (2011), pp.1275-1280.
(11) Fukui, K., et al., "The Improving Technology of the Roll Feeling Based on Visual Performance Characteristics", *Transactions of JSAE* (in Japanese), Vol. 40, No. 5 (2009), pp. 1185-1190.

Figs. 14-22 and Table 1
Reprinted from AVEC '12 Proceedings, Hattori, Y., Asai, S., Tsuchiya, Y. and Limpibunterng, T., Target Vehicle Dynamics During Low-speed Cornering: The Effects of Yaw Velocity and SlipAngle on Driver Perception, © 2012 Society of Automotive Engineers of Japan, Inc., with permission from Society of Automotive Engineers of Japan, Inc.

Yoshikazu Hattori
Research Fields:
- Human-vehicle System and Application to Vehicle Dynamics Design
- Nonlinear Optimum Control
- Adaptive Control

Academic Degree: Dr.Eng.
Academic Societies:
- The Japan Society of Mechanical Engineers
- The Society of Instrument and Control Engineers
- The Institute of Systems, Control and Information Engineers
- Society of Automotive Engineers of Japan

Awards:
- Society of Automotive Engineers of Japan Technological Development Award, 2005
- SICE Award for Outstanding Paper, 2006

Eiichi Ono
Research Field:
- Vehicle Dynamics Control

Academic Degree: Dr.Eng.
Academic Societies:
- The Japan Society of Mechanical Engineers
- Society of Automotive Engineers of Japan
- The Society of Instrument and Control Engineers

Awards:
- SICE Award for Outstanding Paper, 1995
- IFAC Congress Applications Paper Prize, 2002
- Paper Award of AVEC, 2002
- Paper Award of AVEC, 2004
- JSME Medal for Outstanding Paper, 2007

Katsuhiko Fukui
Research Field:
- Driver Behavior Analysis

Academic Societiy:
- Society of Automotive Engineers of Japan

Yuji Muragishi
Research Fields:
- Vehicle Dynamics
- Human Sensitivity Analysis

Academic Societies:
- The Japan Society of Mechanical Engineers
- Society of Automotive Engineers of Japan
- The Japan Fluid Power System Society